

**MASTER**Appendix C

"EXAFS Studies of the Local Atomic Environment in Metal-Metal Glasses", J. Wong, F. W. Lytle, H. H. Liebermann, and L. E. Tanner, Proceeding of Conference on "Metallic Glasses: Science and Technology", Budapest, June (1980).

**DISCLAIMER**

This book was prepared as an account of work sponsored by an agency of the United States Government. Neither the United States Government nor any agency thereof, nor any of their employees, makes any warranty, express or implied, or assumes any legal liability or responsibility for the accuracy, completeness, or usefulness of any information, apparatus, product, or process disclosed, or represents that its use would not infringe privately owned rights. Reference herein to any specific commercial product, process, or service by trade name, trademark, manufacturer, or otherwise, does not necessarily constitute or imply its endorsement, recommendation, or favoring by the United States Government or any agency thereof. The views and opinions of authors expressed herein do not necessarily state or reflect those of the United States Government or any agency thereof.

## **DISCLAIMER**

**This report was prepared as an account of work sponsored by an agency of the United States Government. Neither the United States Government nor any agency Thereof, nor any of their employees, makes any warranty, express or implied, or assumes any legal liability or responsibility for the accuracy, completeness, or usefulness of any information, apparatus, product, or process disclosed, or represents that its use would not infringe privately owned rights. Reference herein to any specific commercial product, process, or service by trade name, trademark, manufacturer, or otherwise does not necessarily constitute or imply its endorsement, recommendation, or favoring by the United States Government or any agency thereof. The views and opinions of authors expressed herein do not necessarily state or reflect those of the United States Government or any agency thereof.**

## **DISCLAIMER**

**Portions of this document may be illegible in electronic image products. Images are produced from the best available original document.**

To appear in the Conference Proceeding :"METALLIC GLASSES:  
SCIENCE AND TECHNOLOGY" 1980 , Budapest, Hungary (in press).

EXAFS STUDIES OF THE LOCAL ATOMIC ENVIRONMENT IN  
METAL-METAL GLASSES

J. Wong, F. W. Lytle\*, H. H. Liebermann and L. E. Tanner\*\*

General Electric Corporate Research and Development 950 6982  
Schenectady, New York 12301

\*The Boeing Company 082 7000  
Seattle, Washington

\*\*Man Labs, Inc. 390 2000  
Cambridge, Massachusetts

ABSTRACT

The interatomic distances and nearest neighbor coordinations of constituent atoms in a series of metal-metal glasses:  $M'_{100-x}M''_x$  where  $M' = \text{Zr, Nb}$ ,  $M'' = \text{Fe, Ni, Cu}$  and  $x$  varies from 30-60 at.%, have been determined using the EXAFS technique in conjunction with the x-ray synchrotron source at Stanford. Fourier transforms of the EXAFS signals clearly indicate there are like as well as unlike atom pairs in the first coordination shell about both the  $M'$  and  $M''$  atoms. The ratio of like and unlike pairs scales linearly with composition and is indicative of random mixing in these binary glasses. The  $M'-M''$  separation are shorter than sum of the Goldschmidt radii and implies chemical interaction between the  $M'$  and  $M''$  atoms.

INTRODUCTION

EXAFS (extended x-ray absorption fine structure) is the oscillatory modulation of the absorption coefficient on the high energy side of an x-ray absorption edge of a constituent atom in a system. These oscillations are now theoretically understood to be a final state electron effect arising from the interference between the outgoing photoejected electron and that fraction of itself that is backscattered from the neighboring atoms. The interference directly reflects of the net phase shift of the backscattered electron in the vicinity of the central excited atom, which is largely proportional to the product of the electron momentum  $k$  and the distance traversed by the electron. The type of central absorbing atom as well as backscattering neighboring atoms (i.e. their positions in the Periodic Table) also play a significant role in the interference event. As a result, EXAFS has now been realized to be a powerful structural tool for probing the

atomic environment of matter<sup>(1)</sup>, particularly since the advent of intense, continuous synchrotron radiation in the x-ray region<sup>(2)</sup>.

In this paper, we will report results obtained for a series of metal-metal glasses:  $M'_{100-x}M''_x$ , where  $M' = \text{Zr}$  and  $\text{Nb}$ ,  $M'' = \text{Fe}$ ,  $\text{Co}$ ,  $\text{Ni}$ ,  $\text{Cu}$ , and  $x$  varies from 30-60 at.%. These binary glasses are chosen for several reasons: (i) the K-edge absorption energies (7-9 KeV for Fe to Cu, 17-18 KeV for Zr and Nb) fall nicely in the energy range of Stanford Positron Electron Acceleration Ring (SPEAR, 4 to  $\geq 20$  KeV); (ii) the K-edges are far apart so that the EXAFS of the light metal is not interfered by the onset of the K absorption of the heavy atom; (iii) the composition range of glass formation usually centers around the middle of the binary system and is much wider (30-60 at.%) than the metal-metallocid systems which fall into a narrow region of  $80 \pm 5$  at.% of metal.

## EXPERIMENTAL

The materials were prepared in the form of a ribbon by quenching a stream of the molten alloy into the surface of a rapidly rotating drum in vacuum<sup>(3)</sup>. The as-cast ribbons were 30-25 microns thick and a few mm wide and are suitable for direct transmission measurement for both Zr, Nb EXAFS. For EXAFS measurements above the absorption edge of Fe, Ni or Cu, which have higher absorption coefficients, the ribbons were thinned to 10-12 microns by careful polishing. EXAFS data were obtained using the EXAFS-I spectrometry at Stanford Synchrotron Radiation Laboratory. Spectra were taken at liquid nitrogen temperature in a double-wall cryostat. Details of the EXAFS apparatus are described elsewhere<sup>(4)</sup>.

## RESULTS AND DISCUSSION

A typical EXAFS spectrum is given in Fig. 1(a) for the case of Zr in  $\text{Zr}_{60}\text{Ni}_{40}$ . After background removal and normalization, the EXAFS signal  $\chi$  is extracted and plotted (Fig. 1(b)) as  $\chi \cdot k$  vs. where  $k = \sqrt{263E}$  is the free electron momentum vector and  $E$  is the energy above the absorption edge energy which for Zr is taken at 17.999 keV<sup>(5)</sup>. This is then Fourier transformed<sup>(6)</sup> to

give a radial structure function in real space. In Fig. 1(c), two clearly resolved radial peaks at  $-2.3\text{\AA}$  and  $2.9\text{\AA}$  are seen which correspond to Zr-Cu and Zr-Zr pairs respectively. The relative magnitude of these peaks varies with composition as shown in Fig. 1(d) for the case of  $\text{Zr}_{70}\text{Ni}_{30}$ . The region in the range  $1.5-3.8\text{\AA}$  is back transformed to k-space<sup>(7)</sup> to isolate back-scattering contribution of atoms from only this region of space. The inverse transform was then fitted with a 2-shell model using the single scattering approximation:

$$x(k) = -\frac{1}{k} \sum_j \frac{N_j}{r_j^2} A_j \sin(2kr_j + \phi_j)$$

$A_j$  is a product of  $t_j(2k) \exp(-2\sigma_j^2 k^2) \exp(-2r_j/\lambda)$  where  $t_j(2k)$  is the amplitude term characteristic only of the backscattering atom, the exponent with  $\sigma_j^2$  is the Debye-Waller term and  $\lambda$  is the mean-free path.  $\phi_j$  is the phase-shift containing contributions from both the central and backscattering atoms, and  $j = 1, 2$ . The inverse EXAFS is  $k^4$  weighted to bring out contribution at higher  $k$  and fitted with a non-linear least-squares regression algorithm using the calculated values amplitude and phase functions of Teo and Lee<sup>(8)</sup>. Details of the fitting are discussed elsewhere<sup>(9)</sup>. Fig. 2 shows a typical fit (triangular points) to the experimental data (solid curve) for the inverse of the Zr EXAFS in the region  $1.5-3.8\text{\AA}$ . The coordination number and interatomic distances so derived for the series of Zr- and Nb-glasses are summarized in Table 1.

Table 1

Interatomic separation (to  $\pm 0.05\text{\AA}$ ) and coordination number derived for metal-metal glasses studied.

System	Interatomic Separation		Coordination Number		
	Zr-Zr	Zr-Zr	$N$	$N_2$	$N_2/N_1$
$\text{Zr}_{70}\text{Cu}_{30}$	2.62	3.13	1.37	4.34	3.22
$\text{Zr}_{60}\text{Bi}_{40}$	2.59	3.18	2.72	4.87	1.79
$\text{Zr}_{70}\text{Bi}_{30}$	2.59	3.12	2.13	5.56	2.62
$\text{Zr}_{40}\text{Cu}_{60}$	2.67	3.13	4.34	3.43	1.79
$\text{Zr}_{60}\text{Cu}_{40}$	2.66	3.09	2.80	4.08	1.63
$\text{Nb}_{40}\text{Zr}_{60}$	2.51	3.42	6.4	2.00	0.45
$\text{Nb}_{50}\text{Zr}_{50}$	2.52	3.42	3.94	2.53	0.64

B.B. Goldschmidt radii: Zr-Fe = 2.84 $\text{\AA}$  Zr-Si = 2.91 $\text{\AA}$   
Zr-Cu = 2.87 $\text{\AA}$  Zr-Si = 2.88 $\text{\AA}$

Compared with sum of the Goldschmidt radii<sup>(10)</sup>, the M'-M" separations are significantly shorter and indicative of chemical interaction of the M'-M" pair. The partial coordination numbers, however, are much lower in value than the x-ray<sup>(11)</sup> or neutron diffraction<sup>(12)</sup> determination on similar metal-metal glasses. This is due to coupling of the Debye-Waller term and or due to harmonic effects of the x-ray source. This effect will be analyzed in detail elsewhere<sup>(9)</sup>. The ratio of  $N_2/N_1$ , however, scales with composition in these glasses and varies linearly with the atomic ratio Zr/T or Nb/T as shown in Fig. 3. The linear relationship which goes through the origin is indicative to random mixing in this binary metal-metal glass in contrast with the metal-metalloid glasses which are chemically order about the metalloid constituent<sup>(1)</sup>.

Finally, we have also measured EXAFS spectrum of the transition metal atom. The Fourier transform of the Ni EXAFS in  $Zr_{70}Ni_{30}$  as given in Fig. 4 and again resolvable radial structure peaks are obtained. Detailed analysis is underway and the combined EXAFS determination as both constituent atoms will aid complete definition of the local structure in these novel amorphous alloys and new experimental data to test the existing theories for glassy metals<sup>(9)</sup>.

#### ACKNOWLEDGMENT

We are grateful for the experimental opportunity at Stanford Synchrotron Radiation Laboratory which is supported by NSF Grant No. DMR 73-07692, in cooperation with the Stanford Linear Accelerator Center and the Department of Energy. Support from the US Department of Energy, Division of Basic Energy Sciences, Materials Science Programs, under Contract DE-AC02-79ER10382 (to JW) and from NSF Grants DMR 74-24261 and 77-12919 (to FWL) are also acknowledged.

#### REFERENCES

- [1] J. Wong, "EXAFS Studies of Metallic Glasses" in "METALLIC GLASSES" Vol I edited by H. J. Guntherodt and H. Beck, Springer-Verlag Publisher, (1980).
- [2] S. Doniach et al. J. Vac. Sci. Technology, (1975), 12, 1123.
- [3] H. H. Liebermann in "Rapidly Quenched Metals III" The Metals

Society, (1979), Vol. 1, p. 34.

[4] B. M. Kincaid, Ph.D. Thesis, Stanford University, (1975).

[5] J. A. Bearden and A. F. Burr, Rev. Mod. Phys. 39, (1967) 125.

[6] D. E. Sayers, E. A. Stern, and F. W. Lytle, Phys. Rev. Lett. 27 (1971) 1204.

[7] E. A. Stern, D. E. Sayers and F. W. Lytle, Phys. Rev. (B) 11, (1975), 4836.

[8] B. K. Teo and P. A. Lee, J. Am. Chem. Soc. 101, (1979) 2815.

[9] J. Wong, F. W. Lytle and H. H. Liebermann, to be published.

[10] V. M. Goldschmidt Trans. Fura. Soc. 25 253 (1929).

[11] H. S. Chen and Y. Wasada, Phys. Solid Stat. A. 51, (1979) 593.

[12] T. Mizoguchi et al., "Rapid Quenched Metals III" The Metals Society (1978) Vol. II, P. 384.

[13] G. S. Cargill III, Solid State Phys. 30 (1975) 227.

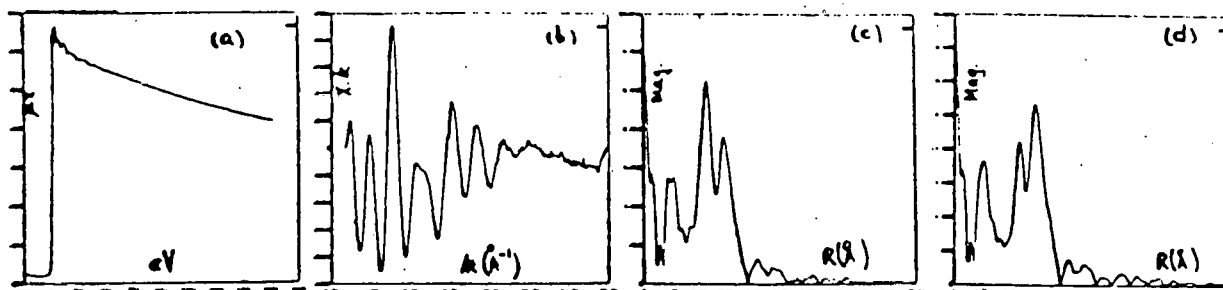


Fig. 1 (a) K-edge absorption spectrum of Zr in  $Zr_{60}Ni_{40}$  glass at 77K  
 (b) Normalized EXAFS plotted as  $X.k$  vs  $k$   
 (c) Fourier transform of (b)  
 (d) Fourier transform of Zr-EXAFS in  $Zr_{70}Ni_{30}$  glass showing changes in the relative peak height at 2.3 and 2.9 Å

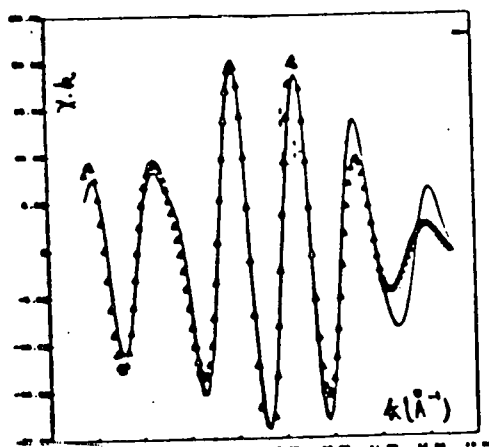


Fig. 2 Inverse transform (solid curve) taken in the range 1.5-3.8 Å from Fig. 1(c) and a fitted spectrum (points)

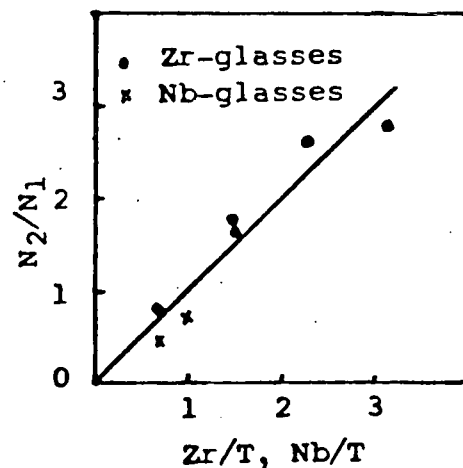


Fig. 3 Plot of ratio of Zr-Zr or Nb-Nb pairs to Zr-T or Nb-T pairs ( $N_2/N_1$ ) vs atomic ratio  $Zr/T$  or  $Nb/T$  in the glass

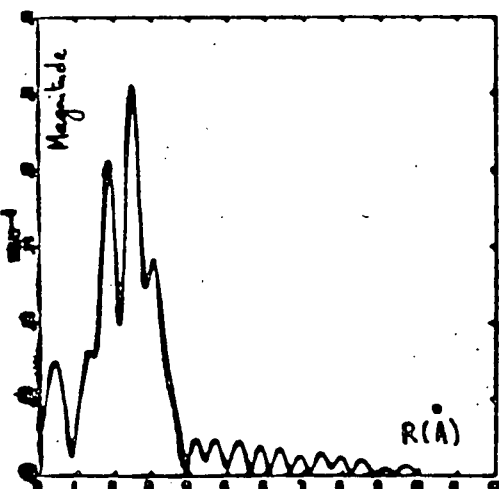


Fig. 4 Fourier transform of Ni EXAFS in  $Zr_{60}Ni_{40}$  glass showing resolution of like and unlike atom pairs in the radial structure function